Nanoscale

ROYAL SOCIETY OF CHEMISTRY

COMMUNICATION

View Article Online
View Journal | View Issue

Cite this: *Nanoscale*, 2025, **17**, 12654

Received 1st January 2025,
Accepted 27th March 2025

DOI: 10.1039/d5nr00002e

rsc.li/nanoscale

Cd_3P_2 QDs emitting in the SWIR through overgrowth of cadmium phosphide clusters†

Nickie Tiwari, Qiaoli Liang and Igor Fedin *

Cd_3P_2 quantum dots (QDs) are promising candidates for short-wave infrared (SWIR) applications. Producing QDs with SWIR emission and sharp spectral features is challenging. In this study, we show that overgrowth of Cd_3P_2 clusters extends the emission of Cd_3P_2 QDs into the SWIR. The resulting QDs are promising for imaging and telecom applications.

Introduction

Materials emitting in the near-IR range of the spectrum (800–1700 nm) have various applications in telecommunications, biomedical imaging, and sensors.[1–3] The three major telecom bandwidths include 800–900 nm, 1200–1360 nm, and 1450–1750 nm.[4] Emitters in the short-wave infrared (SWIR, 1400+ nm) window have garnered interest for telecom and bioimaging owing to the improved penetration in this region.[5] Ideal emitters should have a high quantum yield at a given wavelength as well as little variation in emission energy.[6] Colloidal quantum dots (QDs) are viable candidates for near-IR emitters owing to their tunable emission, facile synthesis,[7–9] and solution-processibility.[10] Several QD compositions that yield near-IR emission such as InAs[11] and lead chalcogenides[12] have been extensively studied. However, there are disadvantages to these materials. Colloidal InAs QDs are prone to anti-site defects due to the close electronegativities of In and As, which impair their emission.[11] Meanwhile, lead chalcogenides have long radiative lifetimes in the microsecond range.[13] As a result, other QD compositions must be explored to form more efficient near-IR emitters. Cadmium phosphide QDs are narrow-gap semiconductor (bulk bandgap of 0.55 eV) nanocrystals that can emit in the near-IR region[14] with the benefit of tunable emission, simple synthesis, and chemical match between cadmium and phosphorus. However, some major disadvantages of Cd_3P_2 are surface traps and size polydispersity.[15–17] Since the bandgap of QDs is size-dependent,[18] polydispersity broadens the emission spectrum.[19–21] For near-IR applications, it is important to produce Cd_3P_2 QDs emitting longer wavelengths while maintaining sharp spectral features. To extend the near-IR emission of Cd_3P_2 QDs, we used atomically defined clusters.

Atomically defined clusters (a.k.a. magic-sized clusters, or MSCs) are a specific arrangement of atoms that exhibit stability.[22,23] They are typically monodisperse and have a precise number of atoms unlike QDs.[22,23] Clusters have been hypothesized to play a role in QD nucleation and growth.[24,25] Documented clusters include crystalline cadmium selenide $(Cd_{35}Se_{20}(X)_{30}(L)_{30}$,[26,27] $Cd_{56}Se_{35}(X)_{42}(L)_{42}$, $Cd_{84}Se_{56}(X)_{56}(L)_{56}$; X = $PhCO_2$, L = $C_4H_9NH_2$), crystalline indium phosphide $(In_{37}P_{20}(RCO_2)_{51})$,[28,29] amorphous cadmium selenide $(CdSe)_{33}$ and $(CdSe)_{34}$;[30,31] and amorphous indium arsenide $(In_{26}As_{18}(O_2CR)_{24}(PR'_3)_3)$.[32–34] Cadmium phosphide clusters were first reported in 2009, but there is limited information

Department of Chemistry and Biochemistry, The University of Alabama, Tuscaloosa, AL, 35487, USA. E-mail: ifedin@ua.edu

†Electronic supplementary information (ESI) available. See DOI: https://doi.org/10.1039/d5nr00002e

Igor Fedin

Igor Fedin is an Assistant Professor in the Department of Chemistry and Biochemistry at The University of Alabama. He received his B.S. in Chemistry from Kyiv National University in 2009, M.S. in Physics from the University of Akron in 2011, and Ph.D. in Chemistry from the University of Chicago in 2017. He was a postdoctoral research associate at Los Alamos National Laboratory in 2017–2020. His research at UA focuses on bright, fast, durable short-wave infrared (SWIR) emitters for telecom applications.

about them. In particular, their chemical formula is unknown.[35] In this study, we further characterize cadmium phosphide clusters and study their applications to grow larger, improved Cd_3P_2 QDs. We demonstrate the conversion of the clusters to Cd_3P_2 QDs and expand it to overgrowth of the clusters over Cd_3P_2 QDs to produce larger Cd_3P_2 QDs to push their emission to the SWIR.

Results and discussion

Synthesis and characterization of cadmium phosphide MSCs

We synthesized cadmium phosphide clusters by reacting cadmium oleate with tris(trimethylsilyl)phosphine (TMSP) in 1-octadecene (ODE) at moderate temperatures (150 °C) under nitrogen. The absorption and photoluminescence (PL) spectra of the resulting MSCs reproducibly showed pronounced peaks at 447 and 455 nm, respectively (Fig. 1a), which is consistent with the previous report on these clusters[35] and results in a small Stokes shift of 48 meV, which is close to the longitudinal optical (LO) phonon of Cd_3P_2.[14]

To further characterize the composition of the MSCs, we measured the MALDI mass spectrometry of Cd_3P_2 QDs and MSCs using the reflectron and linear methods in positive fragmentation modes in the low- and high-mass regions (Fig. 1b–d). In the high-mass region, the MS of Cd_3P_2 QDs showed a distinct band corresponding to the distribution of molecular ions (Fig. 1b), similar to the reported MS of InP QDs.[36] In contrast, MSCs did not show a molecular band or any resolvable peaks beyond 6000 Da (Fig. 1b and c). In the low-mass region, the spectra of the clusters and QDs were comparable and showed numerous fragment peaks (Fig. S1†). The complex isotopic composition of Cd contributes to the broadening of fragment peaks. The average molecular mass of Cd_3P_2 is 399.2 Da and that of $Cd(C_{17}H_{33}CO_2)$ 393.9 Da, both of which could contribute to the repeating units in the spectra. One of the heaviest resolvable fragment peaks has a mass of 5623.4 Da, which we assign to the composition $Cd_{32}P_{20}(C_{17}H_{33}CO_2)_5^+$, which has a predicted mass of 5623.9 Da. Based on the composition of the heaviest fragments, cadmium phosphide MSCs have at least 10 units of Cd_3P_2 (Table 1).

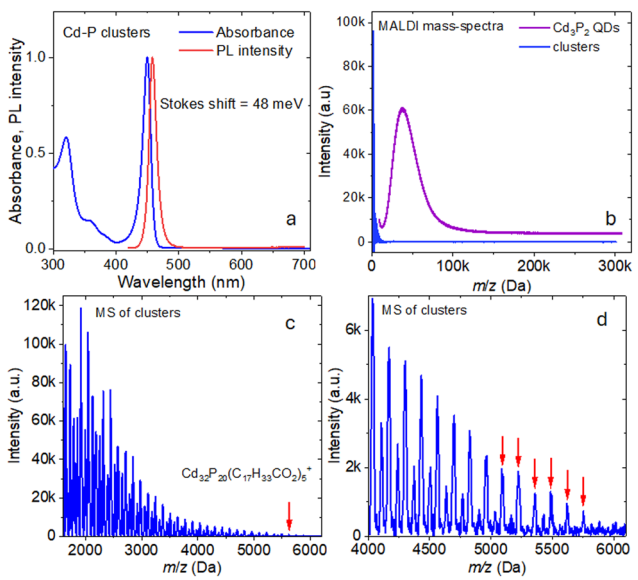

Fig. 1 (a) Absorption and PL spectra of cadmium phosphide magic-sized clusters (MSCs). (b) MALDI mass-spectra of Cd_3P_2 QDs and the MSCs in the high-mass region (c) MALDI MS of the MSCs in the region from 2000 to 6000 Da. The composition of the heaviest identifiable fragment is indicated (d) MALDI MS of the MSCs in the region from 4000 to 6000 Da. The arrows point to the heaviest identifiable fragment peaks.

Evolution of cadmium phosphide clusters into Cd_3P_2 QDs through continuous injection

When we combined $Cd(oleate)_2$, TMS_3P, and ODE at temperatures below 100 °C, we obtained a yellow solution. As we continuously injected this solution into ODE at 180 °C, we took the aliquots throughout the injection and measured their absorption and PL spectra. The MSCs emerged in the solution in the first 5 min, and their population peaked at 10 min after the start of the injection, as indicated by the reproducible absorption peaks (441–447 nm) and emission peaks (451–455 nm) (Fig. 2a and b).

After that, the decrease in the cluster emission peak was accompanied by the emergence of a new peak at 620 nm, its growth, and redshift. The decrease in the MSC luminescence and increase in the near-IR emission indicates that the clusters are converting to Cd_3P_2 QDs with prolonged exposure to heat (Fig. 2). Cadmium phosphide MSCs can be used to grow Cd_3P_2 QDs through heat; however, there are limits to the growth that can be achieved using this method. The largest QDs formed when heating cadmium phosphide clusters emitted at 900 nm.

Overgrowth of cadmium phosphide clusters onto Cd_3P_2 QDs

We used cadmium phosphide clusters to produce larger Cd_3P_2 QDs through overgrowth. It was shown previously that InAs clusters could be used to form monodisperse large InAs QDs through continuous injection into a solution of InAs QDs.[33] Through this method, we aimed to grow larger Cd_3P_2 QDs by

Table 1 Assignment of chemical formulas to the six heaviest fragments observed in the MALDI MS of cadmium phosphide clusters (shown in Fig. 1d)

Fragment formula	Theoretical average mass (Da)	MALDI fragment average mass (Da)
$Cd_{29}P_{17}(C_{17}H_{33}CO_2)_7^+$/ $Cd_{27}P_{15}(C_{17}H_{33}CO_2)_8^+$	5756.6/5751.3	5753.7
$Cd_{32}P_{20}(C_{17}H_{33}CO_2)_5^+$	**5623.9**	**5623.4**
$Cd_{23}P_{12}(C_{17}H_{33}CO_2)_9^+$/ $Cd_{21}P_{10}(C_{17}H_{33}CO_2)_{10}^+$	5490.2/5484.9	5487.9
$Cd_{26}P_{15}(C_{17}H_{33}CO_2)_7^+$/ $Cd_{28}P_{17}(C_{17}H_{33}CO_2)_6^+$	5357.5/5362.8	5359.1
$Cd_{29}P_{18}(C_{17}H_{33}CO_2)_5^+$	**5224.7**	**5224.8**
$Cd_{22}P_{12}(C_{17}H_{33}CO_2)_8^+$/ $Cd_{20}P_{10}(C_{17}H_{33}CO_2)_9^+$	5096.4/5091.1	5093.9

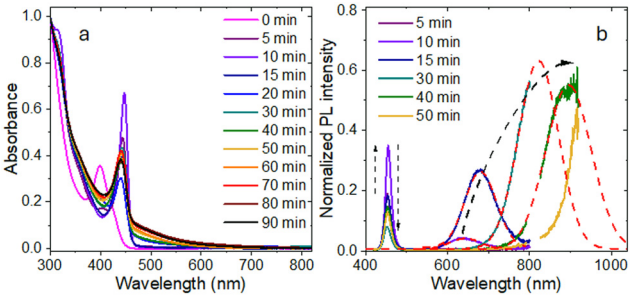

Fig. 2 (a) Absorption and (b) PL spectra of aliquots of the solution of Cd and P precursors in 1-octadecene at 180 °C showing the emergence and decay of cadmium phosphide MSCs.

continuously injecting cadmium phosphide clusters into a solution of Cd_3P_2 QDs in the presence of free oleic acid to prevent the formation of small secondary nucleates.[14] We performed a series of growth experiments on Cd_3P_2 QDs of different sizes. As the injection progressed, we measured optical spectra and the PL quantum yield (PLQY) of the aliquots (Fig. 3, S2,† and Table 2).

For the QDs emitting initially at 965 nm, we observed a red shift in the PL throughout all aliquots, achieving a final emission at 1338 nm (Fig. 3a). The redshift indicates the overgrowth of the clusters on the QD surface likely through Ostwald ripening (dissolution and deposition). The PLQY declined monotonically for the consecutive aliquot and reached 7.3% for the final product. A batch of QDs emitting initially at 1010 nm showed a slight blue shift at the beginning of the injection, likely due to slight etching of the QD surface (Fig. 3b). Subsequently, in aliquots A2 and A3, we observed a

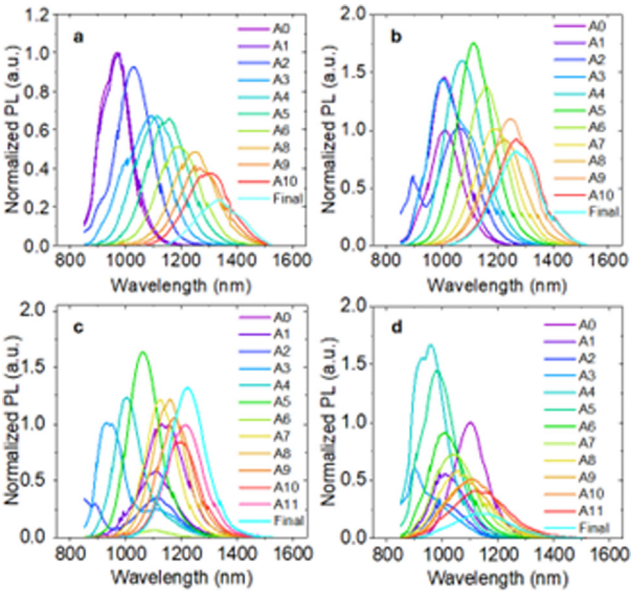

Fig. 3 PL spectra of the aliquots of continuous injection of cadmium phosphide clusters on Cd_3P_2 QDs initially emitting at: (a) 965 nm, (b) 1010 nm, (c) 1102 nm, (d) 1145 nm.

Table 2 Emission wavelengths and PLQYs of the initial, the brightest, and the final aliquots of the overgrowths of cadmium phosphide MSCs onto Cd_3P_2 QDs

Initial λ	Initial QY	λ of the brightest aliquot	QY	Final λ	Final QY
965 nm	22%	965 nm	22%	1338 nm	7.3%
1010 nm	13%	1113 nm	26%	1277 nm	15%
1102 nm	19%	956 nm	31%	1117 nm	6.7%
1145 nm	15%	1055 nm	19%	1224 nm	18%

bimodal distribution. The bluer peak likely resulted from secondary QDs produced from the MSCs while the longer-wavelength peak resulted from the cluster monomers fusing with the surface of the original QD. In subsequent aliquots, the bimodal distribution was gone, and we observed a steady redshift until the QDs reached a final emission at 1277 nm. Initially, the PL intensity increased, reaching a maximum in the fifth aliquot (1113 nm). The aliquots remained brighter than the original QDs until A9 (1245 nm). The PLQY of the final product was 14.8%.

The overgrowths on the 1102 and 1145 nm emitting QDs exhibited similar characteristics (Fig. 2c and d). Initially, we observed a blue shift until A3. Subsequently, there was a red shift in PL for the duration of the continuous injection. The increase in brightness can also be seen in these trials. The optimum brightness was achieved in A4 and A5 for the 1104 and 1145 nm emitting dots. However, the aliquots remained brighter than the original QD until A5 for the 1102 nm emitting QD trial. The 1102 and 1145 nm emitting dots were able to achieve final PL emission at 1117 nm and 1224 nm respectively. The PLQY of the final products of 1102 and 1145 nm emitting QDs overgrowth were 6.7% and 17.6%, respectively. Remarkably, the final product was brighter than the original 1145 nm emitting QDs.

To confirm the growth of the QDs, we took TEM images of the initial QDs and final products of the overgrowth trials of the 1025 nm, 1102 nm, and 1145 nm emitting QDs. All three experiments exhibited growth from the initial to the final product (Fig. 4, Tables 2, S4–5†). For the overgrowth on the 1102 nm emitting QDs, the average QD diameter increased

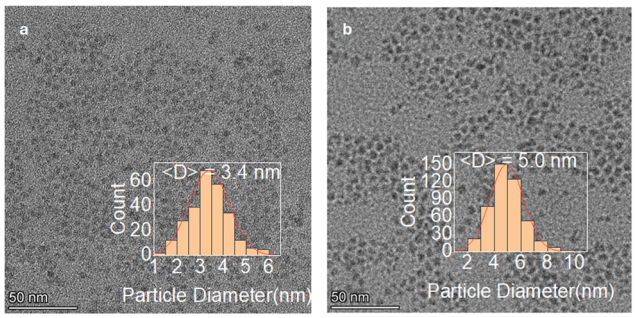

Fig. 4 TEM images of the products of overgrowth on the 1010 nm emitting QDs: (a) initial QDs with average size of 3.4 nm (b) final QDs with average size 5.0 nm.

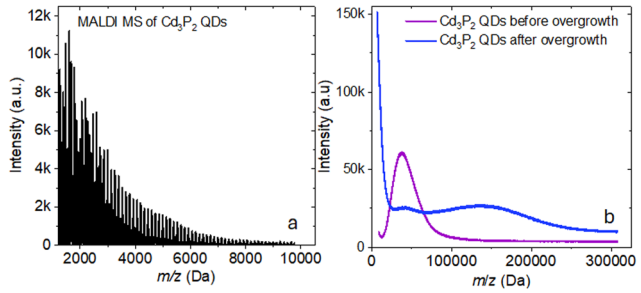

Fig. 5 (a) MALDI MS of Cd_3P_2 QDs emitting at 1010 nm in the low-mass region before cluster overgrowth. (b) MALDI MS of Cd_3P_2 QDs in the high-mass region before and after cluster overgrowth.

from 3.4 nm to 5.0 nm. For the overgrowth on the 1025 nm emitting QDs, the average QD diameter increased from 2.7 nm to 4.4 nm while the average QD diameter increased from 4.1 nm to 5.0 nm for the overgrowth on the 1145 nm emitting QDs.

To further confirm the growth of the QD, we measured MS before and after the cluster overgrowth on the 1010 nm emitting QDs (Fig. 5 and S1†). In the-low mass region, the QDs exhibited peaks up to 10 000 Da (Fig. 5a). We have putatively assigned the heavier fragment to $Cd_{53}P_{33}(C_{17}H_{33}CO_2)_9^+$ (Table S1†). In the high-mass region, we observed a distinct band at 38 000 Da that corresponds to the average molecular weight of the QDs (Fig. 5a). After the overgrowth, the QDs exhibited a bimodal distribution. The peak at 40 000 Da corresponds to the remaining population of the original QDs while the heavier peak at 140 000 Da indicates the growth of the QDs after the cluster overgrowth. Based on the mass of the peaks, the QDs emitting at 1010 nm estimated growth from 2.8 nm to 4.2 nm which agrees with the TEM studies.

Powder X-ray diffraction of a QD sample after the overgrowth confirmed that the tetragonal crystal structure was maintained through the treatment (Fig. S6†). Overall, this set of experiments indicates that cadmium phosphide MSCs enable the growth of brighter QDs emitting in the SWIR. Similar results have been previously achieved with InAs clusters[33] and $CuInSe_2/CuInS_2$ core–shell structures.[37]

Experimental

Synthesis of cadmium phosphide MSCs

To synthesize the clusters, a solution was prepared in the glovebox consisting of 0.30 mmol cadmium oleate, 1.8 ml of 1-octadecene (ODE), and 0.10 mmol tris(trimethylsilyl)phosphine (TMSP). The solution was injected into 6.0 ml of octadecene at 110 °C under N_2. The clusters were precipitated out of the solution with ethanol. The resulting precipitate was dissolved in toluene and stored in the glovebox.

Synthesis of Cd_3P_2 QDs

1.5 mmol cadmium oxide and 5.5 mmol oleic acid were degassed at 110 °C in 20 ml of ODE. A solution 0.145 ml TMSP in 2.5 ml of 1-octadecene was injected under N_2 at various temperatures and reaction times to form QDs of desired emission. To form 965 nm emitting QDs, the TMSP solution was injected at 215 °C for 40 s. To form the 1010 nm emitting QDs, the TMSP solution was injected at 215 °C for 55 seconds. To form the 1102 nm emitting QDs, the TMSP solution was injected at 210 °C and reacted for 90 seconds. To form the 1145 nm emitting QDs, the TMSP solution was injected at 200 °C for 45 s.

Continuous injection cadmium phosphide clusters onto Cd_3P_2 QDs

The cadmium phosphide cluster solution consisted of 6 ml of 0.50 M $Cd(oleate)_2$, 6 ml ODE, and 290 μl TMSP. The Cd_3P_2 QDs (about 20 mg) were dispersed in 1 ml of toluene and added to 6 ml of ODE. The cluster solution was continuously injected at 180 °C under nitrogen.

Mass spectrometry

The Matrix-Assisted Laser Desorption Ionization (MALDI) Time of Flight (TOF) Mass spectrometry (MS) experiments were performed on a Bruker rapifleX mass spectrometer equipped with a Bruker scanning smartbeam™ 3D laser of 355 nm wavelength (≥100 μJ per pulse). For mass calibration in reflectron mode, peptides Angiotensin I, somatostatin-28, and ubiquitin at 1 mg mL^{-1} in water were mixed with 2-nitrophloroglucinol (2-NPG, 50 mM, 50/50 ACN/water, 0.1% trifluoroacetic acid) matrix at 1 : 1 : 1 : 3 volume ratio and 1 μL was spotted on a stainless steel MALDI target. For mass calibration in linear mode, bovine serum albumin protein (6.7 mg mL^{-1} in water) was mixed with 2-NPG matrix at 1 : 9 volume ratio. A solution of clusters and QDs in toluene was mixed with 20 mg mL^{-1} *trans*-2-[3-(4-*tert*-butylphenyl)-2-methyl-2-propenylidene] malononitrile (DCTB) in toluene in a 1 : 1 volume ratio with 1.0 μL applied on the target and dried. The MS spectra were acquired in reflectron positive ion mode for low mass region (1–9 kDa) and linear positive ion mode for high mass region (2–200 kDa) with Bruker flexControl 4.0 and analysed with flexAnalysis 4.0.

Conclusions

With MALDI MS, we found that cadmium phosphide MSCs showed a fragment which we assigned to $Cd_{32}P_{20}(C_{18}H_{33}O_2)_5$, which corresponds to at least 10 units of Cd_3P_2. We demonstrated that these MSCs converted into Cd_3P_2 QDs upon heating. We successfully used cadmium phosphide MSCs to grow SWIR-emitting Cd_3P_2 QDs and enhance the brightness through overgrowth methods. We confirmed the overgrowth with a combination of optical spectroscopy, TEM, and MS. With the success of the overgrowth, we achieved emission in the SWIR. This technique will be useful in developing overgrowth protocols for challenging shell compositions (*e.g.*, InP).

Author contributions

The manuscript was written through the contributions of all authors.

Data availability

All data, including absorption and emission spectra, spectra from integrating sphere measurements, transmission electron micrographs, and mass spectra are available in the ESI.†

Conflicts of interest

There are no conflicts to declare.

References

1 J.-C. G. Bünzli and S. V. Eliseeva, Lanthanide NIR luminescence for telecommunications, bioanalyses and solar energy conversion, *J. Rare Earths*, 2010, **28**(6), 824–842.
2 Y.-T. Yang, Y.-Z. Guo, Z.-C. Shen, J.-L. Liu, R. Yuan and Y.-Q. Chai, AgAuS Quantum Dots as a Highly Efficient Near-Infrared Electrochemiluminescence Emitter for the Ultrasensitive Detection of MicroRNA, *Anal. Chem.*, 2023, **95**(24), 9314–9322.
3 Kenry, Y. Duan and B. Liu, Recent Advances of Optical Imaging in the Second Near-Infrared Window, *Adv. Mater.*, 2018, **30**(47), 1802394.
4 S. N. Bertram, B. Spokoyny, D. Franke, J. R. Caram, J. J. Yoo, R. P. Murphy, M. E. Grein and M. G. Bawendi, Single Nanocrystal Spectroscopy of Shortwave Infrared Emitters, *ACS Nano*, 2019, **13**(2), 1042–1049.
5 W. Liang, S. He and S. Wu, Fluorescence Imaging in Second Near-infrared Window: Developments, Challenges, and Opportunities, *Adv. NanoBiomed Res.*, 2022, **2**(11), 2200087.
6 C. T. Jackson, S. Jeong, G. F. Dorlhiac and M. P. Landry, Advances in engineering near-infrared luminescent materials, *iScience*, 2021, **24**(3), 102156.
7 J. Pichaandi and F. C. J. M. van Veggel, Near-infrared emitting quantum dots: Recent progress on their synthesis and characterization, *Coord. Chem. Rev.*, 2014, **263–264**, 138–150.
8 Y. Ma, Y. Zhang and W. W. Yu, Near infrared emitting quantum dots: synthesis, luminescence properties and applications, *J. Mater. Chem. C*, 2019, **7**(44), 13662–13679.
9 W. Yin, X. Zhang, X. Yang, A. L. Rogach and W. Zheng, Emitter structure design of near-infrared quantum dot light-emitting devices, *Mater. Today*, 2023, **67**, 446–467.
10 M. Bayer, Bridging Two Worlds: Colloidal versus Epitaxial Quantum Dots, *Ann. Phys.*, 2019, **531**(6), 1900039.
11 H. Bahmani Jalali, L. De Trizio, L. Manna and F. Di Stasio, Indium arsenide quantum dots: an alternative to lead-based infrared emitting nanomaterials, *Chem. Soc. Rev.*, 2022, **51**(24), 9861–9881.
12 C. Dong, S. Liu, N. Barange, J. Lee, T. Pardue, X. Yi, S. Yin and F. So, Long-Wavelength Lead Sulfide Quantum Dots Sensing up to 2600 nm for Short-Wavelength Infrared Photodetectors, *ACS Appl. Mater. Interfaces*, 2019, **11**(47), 44451–44457.
13 C. Cheng, J. Li and X. Cheng, Photoluminescence lifetime and absorption spectrum of PbS nanocrystal quantum dots, *J. Lumin.*, 2017, **188**, 252–257.
14 S. Miao, S. G. Hickey, B. Rellinghaus, C. Waurisch and A. Eychmüller, Synthesis and Characterization of Cadmium Phosphide Quantum Dots Emitting in the Visible Red to Near-Infrared, *J. Am. Chem. Soc.*, 2010, **132**(16), 5613–5615.
15 C. Giansante and I. Infante, Surface Traps in Colloidal Quantum Dots: A Combined Experimental and Theoretical Perspective, *J. Phys. Chem. Lett.*, 2017, **8**(20), 5209–5215.
16 A. Jain, O. Voznyy, M. Korkusinski, P. Hawrylak and E. H. Sargent, Ultrafast Carrier Trapping in Thick-Shell Colloidal Quantum Dots, *J. Phys. Chem. Lett.*, 2017, **8**(14), 3179–3184.
17 M. Abdellah, K. J. Karki, N. Lenngren, K. Zheng, T. Pascher, A. Yartsev and T. Pullerits, Ultra Long-Lived Radiative Trap States in CdSe Quantum Dots, *J. Phys. Chem. C*, 2014, **118**(37), 21682–21686.
18 P. K. Khanna, N. Singh and P. More, Synthesis and band-gap photoluminescence from cadmium phosphide nanoparticles, *Curr. Appl. Phys.*, 2010, **10**(1), 84–88.
19 Y. Liu, D. Kim, O. P. Morris, D. Zhitomirsky and J. C. Grossman, Origins of the Stokes Shift in PbS Quantum Dots: Impact of Polydispersity, Ligands, and Defects, *ACS Nano*, 2018, **12**(3), 2838–2845.
20 A. Sharma, C. Mahajan and A. K. Rath, Reduction of Trap and Polydispersity in Mutually Passivated Quantum Dot Solar Cells, *ACS Appl. Energy Mater.*, 2020, **3**(9), 8903–8911.
21 D. Zhitomirsky, I. J. Kramer, A. J. Labelle, A. Fischer, R. Debnath, J. Pan, O. M. Bakr and E. H. Sargent, Colloidal Quantum Dot Photovoltaics: The Effect of Polydispersity, *Nano Lett.*, 2012, **12**(2), 1007–1012.
22 S. Busatto and C. de Mello Donega, Magic-Size Semiconductor Nanostructures: Where Does the Magic Come from?, *ACS Mater. Au*, 2022, **2**(3), 237–249.
23 C. Palencia, K. Yu and K. Boldt, The Future of Colloidal Semiconductor Magic-Size Clusters, *ACS Nano*, 2020, **14**(2), 1227–1235.
24 A. S. Mule, S. Mazzotti, A. A. Rossinelli, M. Aellen, P. T. Prins, J. C. van der Bok, S. F. Solari, Y. M. Glauser, P. V. Kumar, A. Riedinger and D. J. Norris, Unraveling the Growth Mechanism of Magic-Sized Semiconductor Nanocrystals, *J. Am. Chem. Soc.*, 2021, **143**(4), 2037–2048.
25 A. B. Pun, S. Mazzotti, A. S. Mule and D. J. Norris, Understanding Discrete Growth in Semiconductor Nanocrystals: Nanoplatelets and Magic-Sized Clusters, *Acc. Chem. Res.*, 2021, **54**(7), 1545–1554.

26 B. M. Cossairt and J. S. Owen, CdSe Clusters: At the Interface of Small Molecules and Quantum Dots, *Chem. Mater.*, 2011, **23**(12), 3114–3119.
27 A. N. Beecher, X. Yang, J. H. Palmer, A. L. LaGrassa, P. Juhas, S. J. L. Billinge and J. S. Owen, Atomic Structures and Gram Scale Synthesis of Three Tetrahedral Quantum Dots, *J. Am. Chem. Soc.*, 2014, **136**(30), 10645–10653.
28 D. C. Gary, S. E. Flowers, W. Kaminsky, A. Petrone, X. Li and B. M. Cossairt, Single-Crystal and Electronic Structure of a 1.3 nm Indium Phosphide Nanocluster, *J. Am. Chem. Soc.*, 2016, **138**(5), 1510–1513.
29 M. R. Friedfeld, D. A. Johnson and B. M. Cossairt, Conversion of InP Clusters to Quantum Dots, *Inorg. Chem.*, 2019, **58**(1), 803–810.
30 L. G. Gutsev, B. R. Ramachandran and G. L. Gutsev, Pathways of Growth of CdSe Nanocrystals from Nucleant (CdSe)34 Clusters, *J. Phys. Chem. C*, 2018, **122**(5), 3168–3175.
31 S. Kilina, S. Ivanov and S. Tretiak, Effect of Surface Ligands on Optical and Electronic Spectra of Semiconductor Nanoclusters, *J. Am. Chem. Soc.*, 2009, **131**(22), 7717–7726.
32 S. Tamang, S. Lee, H. Choi and S. Jeong, Tuning Size and Size Distribution of Colloidal InAs Nanocrystals via Continuous Supply of Prenucleation Clusters on Nanocrystal Seeds, *Chem. Mater.*, 2016, **28**(22), 8119–8122.
33 T. Kim, S. Park and S. Jeong, Diffusion dynamics controlled colloidal synthesis of highly monodisperse InAs nanocrystals, *Nat. Commun.*, 2021, **12**(1), 3013.
34 S. F. Sandeno, S. M. Krajewski, R. A. Beck, W. Kaminsky, X. Li and B. M. Cossairt, Synthesis and Single Crystal X-ray Diffraction Structure of an Indium Arsenide Nanocluster, *ACS Cent. Sci.*, 2024, **10**(3), 744–751.
35 R. Wang, C. I. Ratcliffe, X. Wu, O. Voznyy, Y. Tao and K. Yu, Magic-Sized Cd3P2 II–V Nanoparticles Exhibiting Bandgap Photoemission, *J. Phys. Chem. C*, 2009, **113**(42), 17979–17982.
36 L. Xie, Y. Shen, D. Franke, V. Sebastián, M. G. Bawendi and K. F. Jensen, Characterization of Indium Phosphide Quantum Dot Growth Intermediates Using MALDI-TOF Mass Spectrometry, *J. Am. Chem. Soc.*, 2016, **138**(41), 13469–13472.
37 J. Ning, Z. Duan, S. V. Kershaw and A. L. Rogach, Phase-Controlled Growth of CuInS2 Shells to Realize Colloidal CuInSe2/CuInS2 Core/Shell Nanostructures, *ACS Nano*, 2020, **14**(9), 11799–11808.